Received: 15 December 2021 | Accepted: 13 October 2022

DOI: 10.1111/1462-2920.16249

RESEARCH ARTICLE

environmental microbiology Applied Microbiology International

Stability of a dominant sponge-symbiont in spite of antibiotic-induced microbiome disturbance

Lara Schmittmann[1] | **Tanja Rahn**[1] | **Kathrin Busch**[1] | **Sebastian Fraune**[2] | **Lucía Pita**[1,3] | **Ute Hentschel**[1,4]

[1]GEOMAR Helmholtz Centre for Ocean Research Kiel, RD3 Marine Ecology, RU Marine Symbioses, Kiel, Germany

[2]Heinrich-Heine-University, Zoology and Organismic Interactions, Düsseldorf, Germany

[3]Institut de Ciències del Mar – CSIC, Marine Biology and Oceanography, Marine Biogeochemistry, Atmosphere and Climate, Barcelona, Spain

[4]Christian-Albrechts-University Kiel, Kiel, Germany

Correspondence
Lara Schmittmann and Ute Hentschel, GEOMAR Helmholtz Centre for Ocean Research Kiel, RD3 Marine Ecology, RU Marine Symbioses, Düsternbrooker Weg 20, Kiel 24105, Germany.
Emails: lschmittmann@geomar.de; uhentschel@geomar.de

Funding information
"la Caixa" Foundation, Grant/Award Number: ID 10010434; Deutsche Forschungsgemeinschaft, Grant/Award Numbers: 417981041, CRC1182-TP B01; Gordon and Betty Moore Foundation, Grant/Award Number: GBMF9352; H2020 Marie Skłodowska-Curie Actions, Grant/Award Number: 847648

Abstract

Marine sponges are known for their complex and stable microbiomes. However, the lack of a gnotobiotic sponge-model and experimental methods to manipulate both the host and the microbial symbionts currently limit our mechanistic understanding of sponge-microbial symbioses. We have used the North Atlantic sponge species *Halichondria panicea* to evaluate the use of antibiotics to generate gnotobiotic sponges. We further asked whether the microbiome can be reestablished via recolonization with the natural microbiome. Experiments were performed in marine gnotobiotic facilities equipped with a custom-made, sterile, flow-through aquarium system. Bacterial abundance dynamics were monitored qualitatively and quantitatively by *16 S* rRNA gene amplicon sequencing and qPCR, respectively. Antibiotics induced dysbiosis by favouring an increase of opportunistic, antibiotic-resistant bacteria, resulting in more complex, but less specific bacteria-bacteria interactions than in untreated sponges. The abundance of the dominant symbiont, *Candidatus* Halichondribacter symbioticus, remained overall unchanged, reflecting its obligately symbiotic nature. Recolonization with the natural microbiome could not reverse antibiotic-induced dysbiosis. However, single bacterial taxa that were transferred, successfully recolonized the sponge and affected bacteria-bacteria interactions. By experimentally manipulating microbiome composition, we could show the stability of a sponge-symbiont clade despite microbiome dysbiosis. This study contributes to understanding both host-bacteria and bacteria-bacteria interactions in the sponge holobiont.

INTRODUCTION

Microbiome homeostasis and stable species interactions are a key requirement for animal health (Manor et al., 2020; Peixoto et al., 2021). From an ecological perspective, holobionts (host organisms and their associated microbes) are considered ecosystems and ecological concepts on species interactions and dynamics apply (Costello et al., 2012; Fierer et al., 2012). Accordingly, animal microbiomes are in a dynamic equilibrium and resistant to a disturbance within a certain range. Beyond that threshold, disturbances, for example, warming in the marine environment (Fan et al., 2013) or antibiotics in the human gut (Strati et al., 2021), can result in dysbiosis, which is defined as a divergence from a healthy microbiome. In a dysbiotic state, species interactions are altered, and the function of the healthy symbiosis is lost, which often translates to disease (Cho & Blaser, 2012). In some cases, the microbiome is resilient and the state of dysbiosis is reversible, while in other cases dysbiosis becomes a new stable state of the microbiome (Sarker et al., 2017). Importantly, species interactions within the holobiont can help to prevent dysbiosis, for example as probiotic bacterial

strains (Robles-Vera et al., 2020), or even reverse dysbiosis as shown during microbiome transplantation (Le Bastard et al., 2018).

Model systems offer experimental routes to simplify processes and approaching questions that are too complex in the environmental context of the organism. In the host-microbe context, a key tool is hosts with a controlled microbiome, either completely germ-free, with a reduced, defined microbiome (gnotobiotic) or lacking a certain symbiont (aposymbiotic). Mice gnotobiotic models have been first established in the 1950s (Pleasants, 1959) and are since applied in medicine, for example, to understand the role of the microbiome in gastric disease (Rooks et al., 2014), or the side effects of antibiotics (Lange et al., 2016; Ng et al., 2013). Experimental models also allow to test the effectiveness of microbiome-based treatments, such as faecal transplants to treat gastric diseases (Ianiro et al., 2020) and to restore dysbiosis after antibiotic treatment (Le Bastard et al., 2018). Traditional symbioses model systems (Douglas, 2019), such as mice, *Caenorhabditis elegans, Hydra*, or *Drosophila melanogaster*, offer established protocols, ease of manipulation and cost-efficiency, while lacking ecological relevance compared to their wild-type organismic counterparts. Emerging models across the tree of life can increase our understanding across animal evolution or in an environmental context (Bosch et al., 2019). Life and much later multicellularity evolved in the ocean, and aquatic ecosystems harbour diverse symbioses across all animal phyla. The *Vibrio*-squid system is one of the most advanced marine symbioses models that is prominent for its few interacting players and the possibility of investigating symbiotic colonization in naturally symbiont-free juveniles (Nyholm & McFall-Ngai, 2021; Visick et al., 2021). Beyond that, few prominent aquatic symbioses model systems have been established, including the Cnidarians *Hydra vulgaris* (Augustin et al., 2012), *Nematostella vectensis* (Mortzfeld et al., 2016), as well as *Aiptasia sp*. for the *Symbodinaceae*-Cnidarian interaction (Bucher et al., 2016; Costa et al., 2021).

The phylum Porifera (sponges) dates back to the Precambrian (Li et al., 1998) and sponge models allow insights into symbioses at the base of animal evolution (Pita et al., 2016). They are filter-feeders and ecologically relevant organisms, for example due to their role in bentho-pelagic coupling and habitat formation (Bell, 2008). Shallow water sponges harbour one of the most complex microbiomes in the marine environment, with 41 different bacterial phyla detected in sponges translating to >3800 operational taxonomic units (OTUs) per sponge species (Thomas et al., 2016). Microbiome density depends on the host species and can be of either low or high microbial abundance (LMA and HMA, respectively) (Gloeckner et al., 2014; Moitinho-Silva et al., 2017). Sponge microbiome composition is first and foremost determined by sponge host species (Easson & Thacker, 2014; Steinert et al., 2017; Thomas et al., 2016) and is thought to be comparatively resistant to environmental conditions (Bell et al., 2018; Campana et al., 2021). However, cases of dysbiosis in sponges have been reported during disease (Blanquer et al., 2016; Luter et al., 2017) and also in the context of climate change (Fan et al., 2013; Posadas et al., 2021).

An experimental sponge model system would facilitate our understanding of host-microbe and microbe-microbe interactions, as well as microbiome stability and colonization dynamics (Pita et al., 2016). One such example is the sponge *Petrosia ficiformis* where colonization of aposymbiotic hosts with a highly specific photoymbiont, *Candidatus* Synechococcus feldmannii, was documented and the effects on the sponge's microbiome were monitored (Britstein et al., 2020; Cerrano et al., 2022). Another promising candidate with a wide distribution along the North Atlantic coast and a closely related sister species in the Pacific is the shallow water sponge *Halichondria panicea* (Erpenbeck et al., 2004). *H. panicea* is an LMA sponge (Gloeckner et al., 2014) with a unique monodominance of a single bacterial species (25%–80% relative abundance in *16 S* rRNA gene amplicon data), recently described as *Candidatus* Halichondribacter symbioticus (Knobloch et al., 2019a). The genome of this Alphaproteobacterium displays key features of a sponge-symbiont, for example, its role in ammonia assimilation, vitamin B12 synthesis and antimicrobial peptide production (Knobloch et al., 2019c). The sponge host has been studied in its natural environment (e.g., Barthel, 1986, 1988; Lüskow, et al., 2019a; Lüskow, et al., 2019b) including the reproductive cycle (Witte et al., 1994). It is amenable to aquarium maintenance and experimentation with adults that spawn in captivity (Amano, 1986; Riisgård et al., 2016), single-osculum explants (Kumala et al., 2021) and primmorphs, that is, cell aggregates from dissociated cells (Lavrov & Kosevich, 2016). A preliminary host genome assembly is available (Strehlow et al., 2022) and de novo transcriptomes have been published in the context of responses to microbial elicitors (Schmittmann et al., 2021) and exposure to crude oil (Vad et al., 2020).

We evaluated the use of antibiotics to generate gnotobiotic or aposymbiotic (i.e., *Ca.* H. symbioticus-lacking) sponges in newly built, germ-free facilities for marine organisms at the Kiel Marine Organism Culture Centre (KIMOCC). We aimed to understand both compositional and abundance-related changes in the sponge microbiome after disturbance by antibiotics. Therefore, we used qPCR as a quantitative method to track bacterial abundance (cDNA and gDNA) with symbiont-specific as well as general bacterial primers, and *16 S* rRNA gene amplicon sequencing to follow taxonomic composition over time. We further asked

whether the microbiome can be reestablished via recolonization with the natural sponge microbiome.

EXPERIMENTAL PROCEDURES

Experimental overview

Three experiments were performed: first, the 'antibiotic exposure experiment' was run to test an antibiotic cocktail for its efficacy to reduce the *H. panicea* microbiome. Second, the 'recolonization by incubation experiment' was performed to study bacterial community dynamics after antibiotic treatment and recolonization where the natural sponge microbiome was administered to the incubation water (see supplementary material for methods and results). Third, in the 'recolonization by injection experiment' recolonization was performed where the natural microbiome was injected directly to the sponge tissue with a syringe. In the main manuscript, we focus on the recolonization by injection experiment due to higher sampling resolution and replication. More details on the materials and methods are deposited on the online platform protocols.io (Schmittmann & Hentschel, 2021; Schmittmann & Pita, 2021).

Sponge collection

H. panicea individuals were collected by snorkelling from Kiel, Germany (54.424705 N, 10.175133 E) in late October 2018 (antibiotic exposure experiment), and in June 2020 (recolonization by injection experiment). Sponges were individually transported in 500 ml bottles and brought to Baltic flow-through tanks at the institute within 2 h after collection for a 1-week acclimation period prior to experiments.

Experimental conditions

The set-up consisted of 500 ml glass flow-through beakers, that were individually connected to aquarium pumps (GHL Doser2) for water exchange (twice the volume per day, 10 ml every ~15 min) with sterile filtered (0.22 μm) artificial seawater. Artificial seawater (TropicMarine) was sterile filtered with a 0.22 μm membrane (Sartorius SM 162 75, 142 mm) into autoclaved 20 L carboys (Nalgene) and regularly plated on MB agar to test sterility. Autoclaved *Nannochloropsis salina* algae were added at a concentration of ~10^5 cells/ml as a food source (Algova, solution from freeze dried powder). For the antibiotic treatment, an antibiotic cocktail was added to the source water from T0 to T4 of the experiment: rifampicin (50 mg/L in DMSO), Nalidixic acid (50 mg/mL in 0.3 M NaOH), ampicillin (50 mg/mL in water), neomycin (50 mg/mL in water), polymyxin B (2 mg/mL in water). We have chosen the antibiotics based on previous studies with the aquatic invertebrates *Hydra, Nematostella* and *Aurelia aurita* (Domin et al., 2018; Franzenburg et al., 2012; Weiland-Bräuer et al., 2015), as well an covering a spectrum of different mechanisms of actions and bacterial targets. From day T4 on, the antibiotic treatment was stopped, and the residual antibiotics were washed out within 1 day (the estimated concentration was monitored by pigmentation of rifampicin). Fresh artificial seawater was prepared every day during the antibiotic treatment and every alternating day afterwards. Experiments were performed with stable temperatures and salinities according to the environmental conditions at the time of the respective experiment (Table S1). In order to control the efficacy of the antibiotic treatment, colony forming units were counted from the seawater. Water from four replicates per treatment was sampled several times throughout the recolonization experiments via a sterile serological 10 ml pipet permanently inserted in the culture units. Dilutions were prepared 1:1000 in sterile 1.5% NaCl, and 100 μl plated onto MarineBroth (Difco2216) agar plates in triplicates. After incubation at 28°C for 7 days, colony forming units were counted.

Gnotobiotic experimental facilities

Experiments were performed in marine gnotobiotic chambers that are inspired by gnotobiotic mouse facilities. A detailed description of the setup and materials used is provided on the online platform protocols.io (Schmittmann & Hentschel, 2021). Briefly, they consist of a restricted transitioning area, a preparation climate chamber, and an experimental climate chamber permanently equipped with an air filtration system (CP Type 500 NATURE SYSTEM, Expansion Electronic SRL, Italy) that successfully removes microbes from the air. Further, surfaces were sterilized daily (Curacid Medical wipes, PICO-Medical, Germany), and all materials were either sterile packed, autoclaved or sterilized with ethanol. An experimental aquarium set-up was custom made that enables a sterile flow-through of water and automatic water exchange. To our best knowledge this is the first designated marine gnotobiotic facilities with a sterile flow-through culture system designed for marine sponges. Sponges require high rates of water exchange and animals cannot be kept in for example, petri dishes as was done for *Ciona intestinalis* (Leigh et al., 2016). In previous efforts, antibiotics have been mainly applied to sponge explants (De Caralt et al., 2003), sponge larvae (Gloeckner et al., 2013) or primmorphs (Richardson et al., 2012; Schippers, 2013; Sipkema et al., 2003). The advantage of our proposed

system is the possibility to experiment with adult sponges, which may be a more realistic simulation of sponge performance in their native habitat than tissue or cell culture efforts.

Antibiotic exposure experiment

For the antibiotic exposure experiment, four sponge individuals were each cut into three clones with a sterile scalpel (each about 2 × 2 × 2 cm). One clone per individual was immediately preserved in RNAlater (incubated overnight at 4°C and stored at −80°C) and serves as the start sample T0 ($n = 4$). The other two clones per individual were placed in separate glass beakers and either treated with an antibiotic cocktail from T0 to T4 or served as a control. After a recovery phase of 7 days, tissues were preserved in RNAlater (T11, $n = 4$).

Recolonization experiment

Sixteen sponge individuals were each cut to three clones with a sterile scalpel (each about 4 × 4 × 4 cm). One clone per individual was immediately preserved in RNAlater and serves as the start sample T0 ($n = 16$). The other two clones per individual were each placed in separate glass beakers and all were treated with the antibiotic cocktail described above (note that in this experiment all sponges and clones were treated with antibiotics). DNA extraction and qPCR were performed on the sampling day allowing a real-time tracking of all bacteria and *Ca.* H. symbioticus abundances. Therefore, after the antibiotic treatment, daily biopsy samples were taken from six random tanks by cutting a small tissue piece (~5 × 5 × 5 mm) with sterile scissors while the individual remained within the experiment. On day T12 and T13, half of the sponges were recolonized three times within 36 h. For each recolonization, 2 ml freshly prepared *H. panicea* symbiont inoculum were injected with sterile syringes (0.6 mm diameter, 80 mm length). The control group received a sham injection with sterile-filtered seawater to simulate the injection without transferring bacteria. The bacterial inoculum was prepared by differential centrifugation from several fresh and untreated sponges kept for 19 days in a Baltic flow-through system with a modified protocol after Wehrl et al. (2007) (for further details see supplementary materials). The volume of the sponge tissue used to prepare the inoculum was equivalent to the volume of the sponges to be recolonized (estimated by size). For DNA extraction, the inoculum was pelleted and flash frozen in liquid nitrogen. After recolonization, biopsy samples of sponges were taken daily ($n = 3$), and a larger sampling size ($n = 8$) was taken 2 days and 6 days after recolonization.

DNA/RNA extraction

DNA was extracted from ~25 mg sponge tissue or half of the water filters with the DNeasy PowerSoil Kit (Qiagen, Netherlands). The pelleted inoculum was extracted with the Blood + Tissue Kit (Qiagen, Netherlands) following the manufacturers protocol with proteinase K incubation for 30 min. The DNA was eluted in 50 µl elution buffer. Total RNA from 70–80 mg sponge tissue was extracted with the RNeasy Mini Kit (Qiagen, Netherlands) and RNA eluted in 60 µl. Degradation of RNA was inhibited (1 U/µl SUPERase-IN, Thermo Fisher Scientific, USA) and genomic DNA was removed after extraction (DNA-free DNA removal Kit, Thermo Fisher Scientific, USA). DNA and RNA were quantified in Qubit (DNA and RNA BS and HS Kits, Thermo Fisher Scientific, USA) and checked with NanoDrop (Thermo Fisher Scientific, USA, some RNA samples additionally with Experion, Bio-Rad, USA).

Quantitative real-time PCR (qPCR)

Overall bacterial abundance as well as *Ca.* H. symbioticus abundance was estimated by qPCR based on the *16 S* rRNA gene (Table S2). General bacterial primers were previously applied in sponges to estimate total bacterial abundance (Bayer et al., 2014) while *Ca.* H. symbioticus specific primers were designed for this study (Schmittmann & Pita, 2021). Analysis was run on both gDNA and cDNA (RNA transcribed with iScript cDNA synthesis kit, Bio-Rad). For quantification of gene copy numbers, dilutions of purified PCR products in tRNA solution (10 ng/µl Sigma Aldrich, Germany) were used as standards. The concentration of the highest standard of each dilution series was measured with Qubit (DNA and RNA HS Kits, Thermo Fisher Scientific, USA) and copy numbers calculated based on concentration and fragment length. Quantitative PCRs were performed in a CFX96 real-time detection system (Bio-Rad, Germany) with the Maxima SYBR Green 2x Master Mix (Thermo Fisher Scientific, USA) (Table S3). Standards were run in duplicates and samples in triplicates. Efficiencies and copy numbers were calculated with the Bio-Rad CFX Manager Software (version 3.1) and data analysis was performed in R (version 3.5.1, packages stats, car and rcompanion). Generalized linear models or linear mixed effect models were applied according to the tested data set (Tables S9–S11).

Amplicon sequencing

The V3-V4 variable regions of the *16 S* rRNA gene were amplified in a one-step PCR using the primer pair 341F-806R (dual-barcoding approach [Kozich

et al., 2013]; primer sequences: 5'-CCTACGGGAGGCAGCAG-3′ & 5'-GGACTACHVGGGTWTCTAAT-3′). After verification of the presence of PCR-products by gel electrophoresis, normalization (SequalPrep Normalization Plate Kit; ThermoFisher Scientific, Waltham, USA) and equimolar pooling was performed. Sequencing was conducted on the MiSeq platform (MiSeqFGx; Illumina, San Diego, USA) with v3 chemistry. The settings for demultiplexing were 0 mismatches in the barcode sequences.

Amplicon bioinformatic and statistical analyses

Bioinformatic analyses followed a published protocol (Busch et al., 2022). For computation of microbial core-diversity metrics, sequences were processed within the QIIME2 environment (version 2018.11, Bolyen et al., 2019). Amplicon Sequence Variants (ASVs) were generated from forward reads (truncated to 270 nt) with the DADA2 algorithm (Callahan et al., 2016). Phylogenetic trees were calculated based on resulting ASVs with the FastTree2 plugin with the default parameters (maximum relative frequency of gap characters = 1, minimum relative frequency of non-gap characters = 0.4). Representative ASVs were classified using the Silva 132 99% OTUs *16 S* rRNA gene database (Quast et al., 2013) with the help of a primer-specific trained Naive Bayes taxonomic classifier. Mitochondrial and chloroplast reads were removed. The data were rarefied to a sampling depth of 3300 reads per sample (Figure S2, S3 and S8). Alpha and beta diversity indices (e.g., Faith's Phylogenetic Diversity and weighted UniFrac distances, respectively) were calculated within QIIME2. To evaluate sample separation in ordination space, non-metric multidimensional scaling (NMDS) was performed on weighted UniFrac distances. Alpha diversity was analysed in R (version 3.5.1, packages stats, car and rcompanion) with generalized linear or linear mixed models depending on the dataset (Table S12–S14). Beta diversity (weighted unifrac distances) were tested for dissimilarity by PERMANOVA with 999 permutations and for homogeneity by PERMDISP within QIIME2 (version 2018.11) (Table S4–S8). The dataset was analysed as a whole (T0–T19), as well as a subset only including control and recolonized sponge samples after recolonization (T14–T19).

To assess the effect of recolonization on microbiome community composition, significantly different abundance of ASVs between recolonized and control sponges was assessed for the end of the experiment at T19 (LEfSe in Galaxy version 1.0) (Segata et al., 2011). With an UpSetR analysis 'persister' ASVs (present throughout the whole experiment), and potential 'recolonizer' ASVs (present in inoculum and recolonized sponges only) were identified (UpSetR version 1.4.0) (Conway et al., 2017). The ASV sequences were compared to the GenBank standard database with BLASTN under default parameters and results sorted by e-value (accessed in August 2021). If there were several closest hits with the same e-value, the results were screened for host-association and the closest host-associated hit was reported.

Bacterial co-occurrence networks

Bacterial co-occurrence networks were calculated based on relative abundances with the SparCC methodology (Friedman & Alm, 2012) in SCNIC (version 2020.10) (Shaffer et al., 2022) within QIIME2 (version 2020.8). Significant interactions were defined as $-0.5 > R > 0.5$. Networks were calculated from data subsets to represent different states of the *H. panicea* microbiome: i) *untreated* from the wildtype start samples T0, and ii) *recolonized* from the recolonized sponges T14-T19, compared to *control* from the non-recolonized control sponges. Details on network results can be found in the supplements (Table S16-S21).

Data visualization

Plots were generated in R (version 3.5.1 and 4.0.2, packages ggplot2, plotrix, svglite), but the fluid barplots were prepared in RawGraphs (version 2.0 beta) (Mauri et al., 2017) and the co-occurrence networks were visualized and annotated in Cytoscape (version 3.8.2) (Shannon et al., 2003). If necessary, figure layouts were finalized in Inkscape (version 0.92).

RESULTS

In this study we aimed to remove the bacterial microbiome of *H. panicea*, targeting specifically the dominant symbiont *Ca.* Halichondribacter symbioticus. The *Ca.* H. symbioticus amplicon sequence identified in this study (amplicon sequence variant, ASV 350235dc06427fbe808d1bb3452afc91) is identical to most published sequences from previous studies (0–1 bp difference from 270 bp), (Althoff et al., 1998; Knobloch et al., 2019a; Naim et al., 2014). We designed specific *16 S* rRNA gene primers for *Ca.* H. symbioticus to assess absolute abundance via qPCR and used general bacterial *16 S* rRNA gene primers to quantify total bacterial abundance. The relative proportion of *Ca.* H. symbioticus *16 S* rRNA gene in the total bacterial *16 S* rRNA gene pool estimated by both qPCR and *16 S* rRNA gene amplicon sequencing was highly correlated (Figure S1, $R^2 = 0.87–0.93$). Further, qPCR results from both genomic DNA (gDNA) and complementary DNA

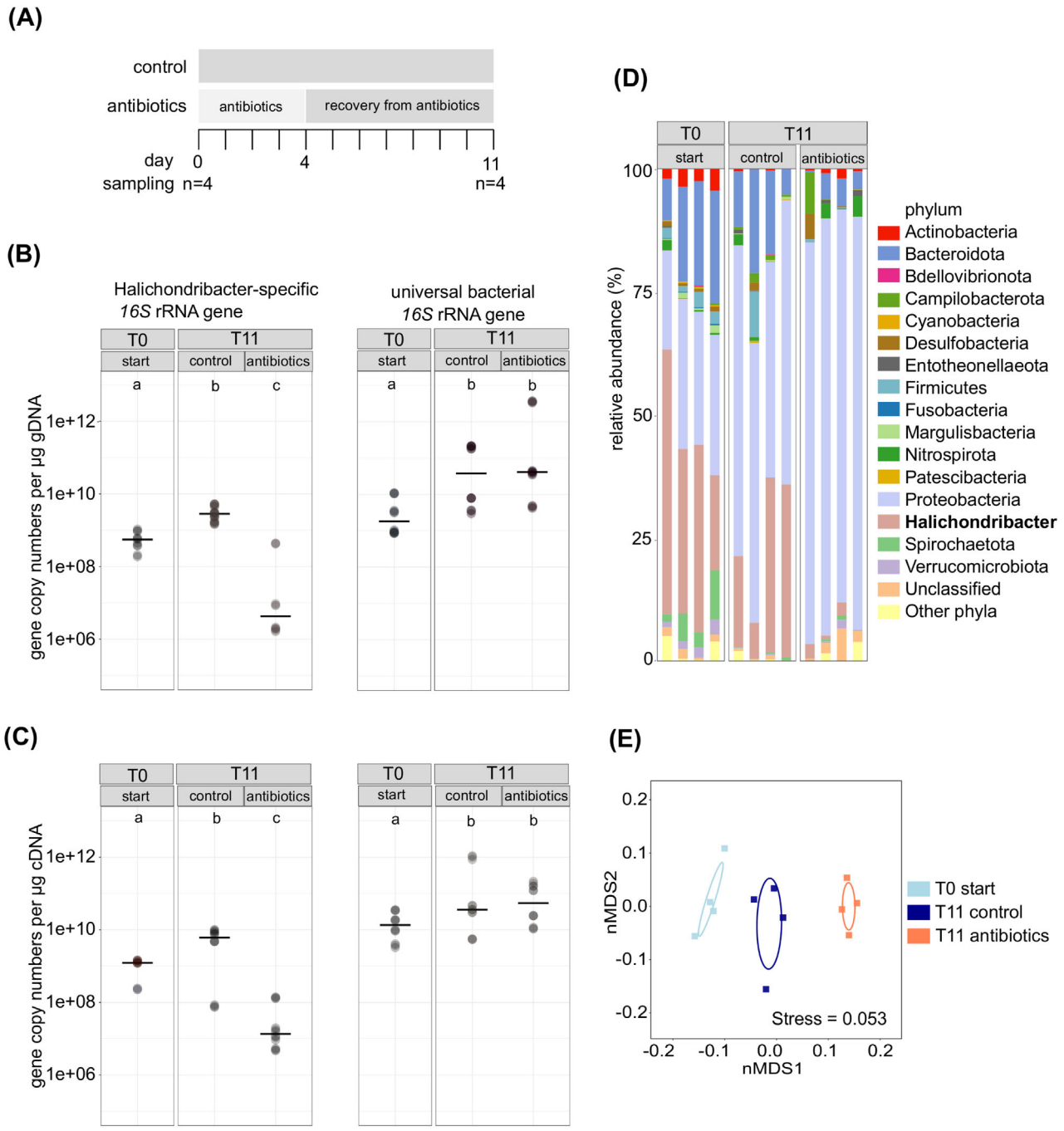

FIGURE 1 (A–E) Antibiotic exposure experiment: Absolute and relative bacterial abundance after antibiotic treatment. (A) Timeline of antibiotic exposure experiment. Sponges were either treated with antibiotics for 4 days or left untreated as a control. Samples were taken prior to the experiment at T0, and after a recovery phase at T11. $n = 4$. (B, C) absolute bacterial abundance estimated by RT-qPCR. *16 S* rRNA gene copy numbers per µg genomic DNA (B) and per µg cDNA (C) at the start (T0) and after the recovery phase (T11). Left: Gene copy numbers for *Ca.* Halichondribacter-specific *16 S* rRNA gene, right: Gene copy numbers for total bacterial *16 S* rRNA gene. Values with different letters are significantly different ($p < 0.05$), and black lines represent median. (D) Relative microbial community composition on phylum level (top 15 phyla) across timepoints and treatments. Proteobacteria are resolved in the Alphaproteobacterium *Ca.* Halichondribacter symbioticus and other Proteobacteria. (E) Non-metric multidimensional scaling plot on weighted UniFrac distances. Colour indicates the treatment and timepoint.

(cDNA; synthesized from RNA) revealed similar trends throughout the experiments (Figure 1B,C, Figure S7), suggesting that the dominant symbiont *Ca.* H. symbioticus and other bacterial microbiome members were active.

Antibiotic exposure experiment

Microbiome changes in *H. panicea* were assessed 7 days after antibiotic treatment (Figure 1A). The absolute abundance of the dominant symbiont *Ca.*

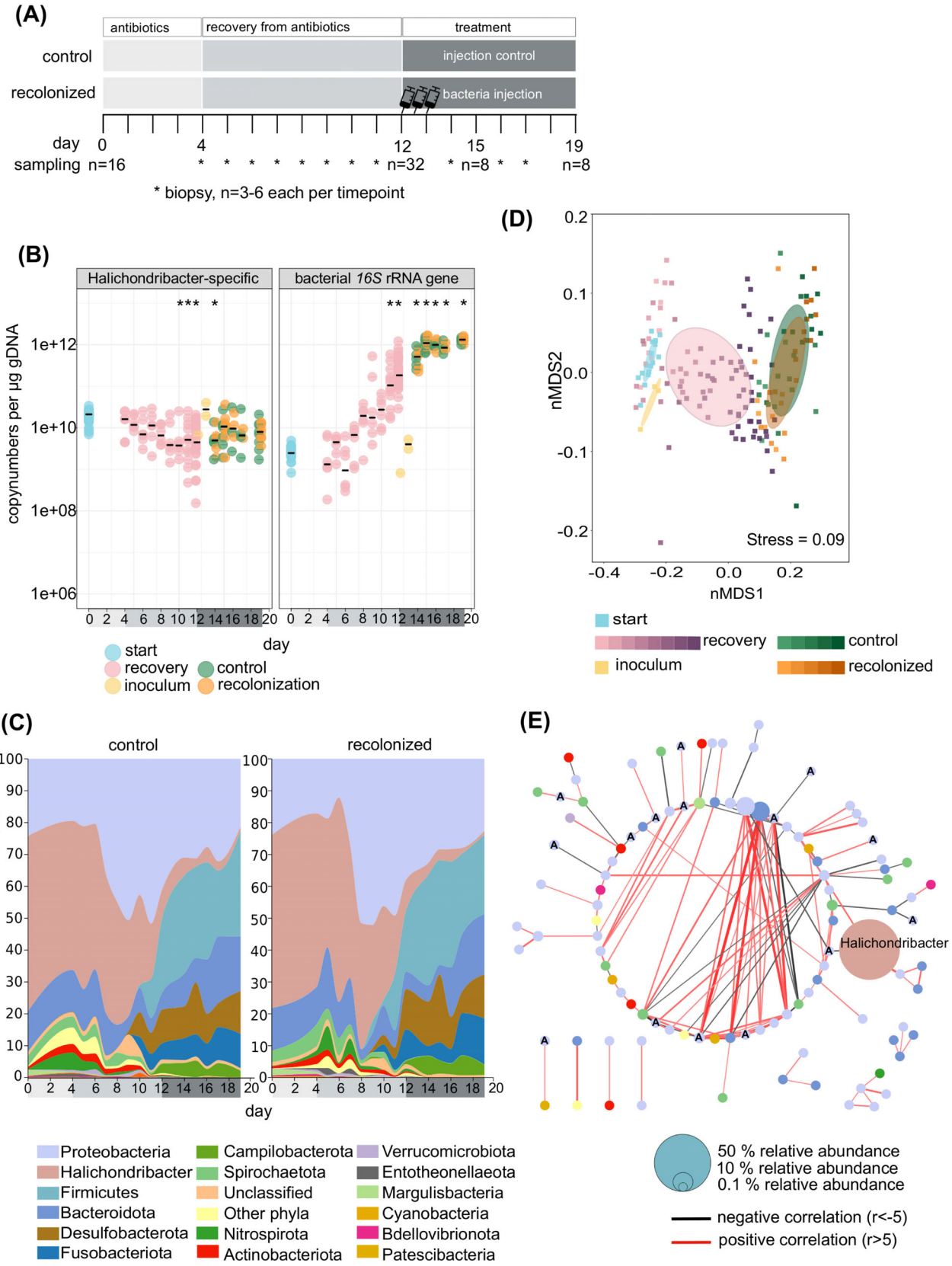

FIGURE 2 Legend on next page.

H. symbioticus increased in the control treatment, respective to T0, while it decreased by 2–3 orders of magnitude after antibiotic treatment, as assessed by qPCR on gDNA level (ANOVA, F-value [2, 31] = 74.81, *p*-value <0.0001) (Figure 1B). The absolute abundance of total bacteria increased significantly, by 1–2 orders of magnitude, in control and antibiotic treated sponges (ANOVA, F-value [2, 33] = 10.17, *p*-value <0.001). Results from cDNA followed similar patterns (ANOVA, F-value [2, 32] = 22.98, *p*-value <0.0001; F-value [2, 33] = 4.06, *p*-value <0.05, respectively) (Figure 1C). With respect to the relative abundance (amplicon sequencing), *Ca.* H. symbioticus ASV numbers decreased from 36.2% ± 7.1% to 1.6% ± 0.7% (average ± standard error) after antibiotic exposure while relative numbers remained at an average of 24.1% ± 6.9% in controls ($n = 4$, Figure 1D). Other Proteobacteria (including *Alteromonadales* and *Vibrionales*) increased in relative abundance over time (from 26.5% ± 2.3% to 82.5% ± 1.1%), regardless the treatment. The composition and beta diversity of the microbial communities shifted in the control sponges (PERMANOVA, pseudo-F = 2.7, adjusted *p*-value <0.03), and even more so, in the antibiotic treated sponges (pseudo-F = 14.13, adjusted *p*-value <0.03) while control and antibiotic treated sponges were significantly different at T11 (pseudo-F = 5.28, adjusted *p*-value <0.03) (Figure 1E, Table S4). The alpha-diversity in terms of evenness (Pilou) and richness (Shannon Diversity) did not change throughout the experiment, whereas phylogenetic diversity (Faith's) decreased significantly in both control and antibiotic treatment (ANOVA, F-value [2, 9] = 12.89, *p*-value <0.01) (Figure S2).

Recolonization experiment

We performed two follow-up experiments to test whether *Ca.* H. symbioticus numbers could be recovered after antibiotic treatment by recolonization with the natural sponge microbiome. The two experiments differed in the mode of recolonization. In the first experiment, the symbiont inoculum was added to the water (incubation) while in the second, the symbiont inoculum was injected into the sponge tissue (injection). We will focus on the injection experiment here (Figure 2A), since the mode of recolonization did not affect the main outcome of the experiments (see supplementary materials for details on the recolonization by incubation experiment), and the temporal resolution and replication is much higher for the recolonization by injection experiment.

When looking at the dynamics of absolute bacterial numbers over time (qPCR), the absolute abundance of *Ca.* H. symbioticus was lower and more variable across individuals than at T0 (Figure 2B). The abundance of *Ca.* H. symbioticus significantly decreased temporarily after antibiotic treatment (Scheirer-Ray-Hare test, H-value [14, 40] = 38.34, *p*-value <0.001), while the drop by 1–2 orders of magnitude was less than the decrease by 2–3 orders of magnitude observed in the antibiotic exposure experiment (Figure 1B). Post-hoc testing revealed that the significant decrease compared to T0 happened between days T10 to T14. From T14 onwards, *Ca.* H. symbioticus absolute numbers recovered to T0 levels, regardless of whether the sponges were recolonized or not (Figure 2B). In contrast, the total bacterial abundance increased during the experiment by three orders of magnitude (Scheirer-Ray-Hare test, H-value [14, 40] =138.77, *p*-value <0.000001). In particular, bacterial *16 S* rRNA gene copy numbers steeply rose in the time frame from T07 to T15, after which a new, stable carrying capacity was reached, independently of whether the sponges were recolonized or not (Figure 2B).

When looking at relative microbial community compositions over time (amplicon sequencing), no differences between recolonized sponges and control sponges were observed (Figure 2C). Both profiles

FIGURE 2 (A–E) recolonization experiment: Absolute and relative bacterial abundance before and after recolonization by injecting the natural microbiome of *H. panicea* to antibiotic treated sponges. (A) Timeline of recolonization by injection experiment. All sponges were treated with antibiotics for 4 days and recovered in sterile filtered artificial seawater for 7 days. Then, sponges were either injected three times with a bacterial inoculum, or sterile-filtered seawateras a sham control on day T12 and T13. Samples were taken prior to the experiment at T0 ($n = 16$), after a recovery phase (before injection) at T12 ($n = 32$), from the bacterial inoculum, and 2 and 6 days after the last recolonization ($n = 8$). In between major samplings, daily biopsy samples were taken ($n = 3$–6). (B) Absolute bacterial abundance estimated by RT-qPCR. *16 S* rRNA gene copy numbers per μg genomic DNA throughout the experiment. Results for *Ca.* Halichondribacter-specific *16 S* rRNA genes (right) and total bacterial *16 S* rRNA genes (left). Different treatment groups are indicated by colour. Black lines represent median per day. Significant differences between the start (T0) and the respective days are indicated by asterisks above the days (ANOVA or Schreier-ray-hare test). Recolonization had no effect on copy numbers, while the sponge individual did affect Halichondribacter-specific copy numbers ($p = 0.00017$). (C) Relative bacterial community composition shown on phylum level (top 15 phyla) across time and separated by treatment. Proteobacteria are resolved in the Alphaproteobacterium *Ca.* Halichondribacter symbioticus and other Proteobacteria. (D) Beta diversity of microbial communities (non-metric multidimensional scaling plot on weighted UniFrac distances). Treatments are represented by colour, with increasing colour intensity representing progressing time. For results of pairwise PERMANOVA on beta diversity see table S7. (E) Bacterial co-occurrence network for untreated wildtype (T0) sponges. Co-occurrences between ASVs ($-0.5 > R > 0.5$, *p*-value <0.05) are displayed by edges (interaction) connecting nodes (ASVs). The colour of the edges depicts the direction of the correlation (negative or positive), and thickness the interaction strength. The size of the nodes is proportional to the relative abundance of ASVs and the colour represents taxonomic affiliation (as in C). ASVs that have the family *Amylibacter* as the closest known relative are labelled 'A'.

changed in similar manner throughout the experiment. The relative abundance of *Ca.* H. symbioticus decreased from 54% ± 1.8% at T0 ($n = 16$) to 1.4% ± 0.4% and 1.2% ± 0.2% in the control and recolonized treatment ($n = 9$), respectively, in the end of the experiment. Certain microbial phyla (mainly Proteobacteria, followed by the phyla Firmicutes, Desulfobacteria, Campilobacteria and Fusobacteria) increased while other bacterial phyla that almost disappeared (among them Actinobacteria, Verrucomicrobiota and Cyanobacteria). Overall, the microbial community was dominated by several phyla at the end of both treatments rather than the monodominance of Proteobacteria at T0, which was reflected in higher evenness (ANOVA, F-value [14, 141] = 21.75, p-value <0.000001) (Figure S3). Both Shannon diversity (richness) and phylogenetic diversity (phylogenetic richness) were more variable after antibiotic treatment than at T0 (Figure S3). Shannon diversity increased until the end of the experiment (Scheirer-Ray-Hare, H-value [12, 136] = 26.26, p-value <0.01), while phylogenetic diversity decreased over time (Scheirer-Ray-Hare, H-value [12, 136] = 43.31, p-value <0.0001). The microbial community compositions (beta diversity) shifted (PERMANOVA, F-value = 26.06, p-value <0.001) from the start to the recovery phase to the treatment, where control and recolonized samples overlapped (Figure 2D). Noteworthy, the inocula were most similar to the starting sponge microbiomes, reflecting a high proportion of *Ca.* H. symbioticus in these samples. Bacterial co-occurrence networks indicate that *Ca.* H. symbioticus is largely independent from the remaining microbiome (3 from total 151 interactions) in untreated sponges (Figure 2E). About 15% of all nodes in the bacterial co-occurrence network were annotated as *Amylibacter*, the closest known relative of *Ca.* H. symbioticus. Some of *Amylibacter* ASVs were among the most connected, while others had only one or few interactions.

We also compared the differences between treatments on a sponge individual basis (Figure S4). This was possible because the same individual was split into two clones that were subjected to either control or recolonized treatment. Interestingly, even after 19 days of experimentation, the abundance of *Ca.* H. symbioticus was nearly identical between clones, and regardless of treatment. Moreover, the sponge individuals followed different trajectories over time: while symbiont populations remained stable in some individuals, they were either increasing or decreasing in others. Notably, the clones of the same individual followed the same trend, which was independent of the treatment regime (Figure S4).

In addition to cultivation-independent analyses (amplicon sequencing, qPCR), we monitored the culturable microbial fraction (Figure S5) which does not represent the complete microbial diversity since most sponge-associated bacteria including *Ca.* H. symbioticus are not culturable (Knobloch et al., 2019b; Wichels et al., 2006). First, we checked for bacterial growth in the culture seawater by counting colony forming units (CFU's). Colony growth was absent during the antibiotic treatment, however bacterial numbers increased in the recovery phase until they reached a plateau of $\sim 10^5$ CFUs/ml at T11. There was no difference between control and recolonized treatments. Secondly, we separately tested the five antibiotics of the cocktail for their inhibition of bacterial growth. Sponge-associated bacteria isolated from antibiotic-treated animals had developed more resistances than those isolated from sponges not treated with antibiotics. These antibiotic-resistant isolates were mainly affiliated to Flavobacteria. All isolated strains remained sensitive to rifampicin, one of the five components of the treatment cocktail.

Identification of persisters and recolonizers

We then inspected the overlap of ASVs that were shared between experimental groups (Figure 3A,B). We defined 'persisters' as those ASVs that were present in all experimental groups ($n = 13$). Persister ASVs were either present in all groups ($n = 11$) or in all groups except inoculum ($n = 2$). Cumulatively, these were also the most abundant ASVs (75% at T0 and 21% at T19), (Figure 3 C). Interestingly, the closest relatives of the persister ASVs were found to be host-associated, and majorly sponge-associated (Table 1). As expected, *Ca.* Halichondribacter symbioticus (P1) belonged to the persisters and was identified in all analysed samples. Two additional persisters (P2: Bacteroidota, Cyclobacteriaceae; P3: Gammaproteobacteria, HOC36) were present in more than half of the replicate sponges throughout the entire experiment. It is noteworthy that persisters were detected in more sponge individuals at the end compared to the beginning of the experiment.

We defined the group of 'recolonizers' as those ASVs that occurred both in the inoculum and the recolonized sponges, while being absent in the control sponges ($n = 8$) (Figure 3). The corresponding ASVs were present in low abundances in the inoculum (0.01%–0.44%) and in untreated sponges (0%–0.86%). Four potential recolonizers were detected in more than half of the replicate sponges (Table 1). Those were affiliated with marine, environmental taxa members, and reached average relative abundances of 8.72% for Bacteroidota, 0.36%–1.29% for Campilobacterota, and 0.18% for Desulfobacterota (Figure S6).

We investigated if and how recolonizers affected bacteria-bacteria interactions by calculating bacterial co-occurrence networks for control and recolonized

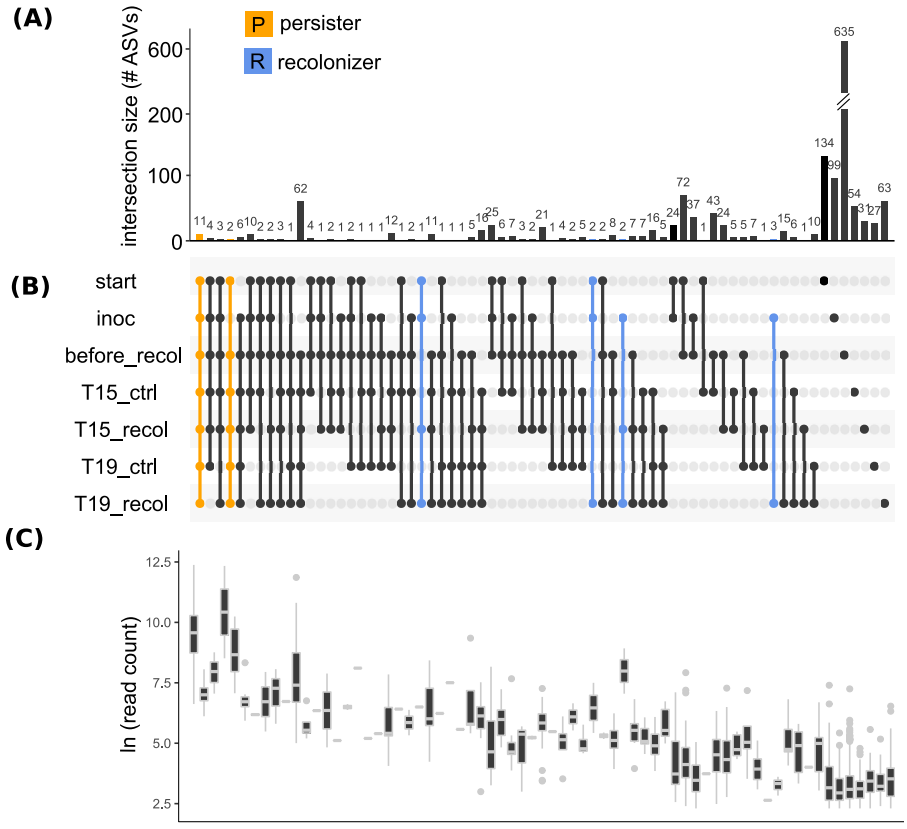

FIGURE 3 Recolonization experiment: Shared ASVs between experimental groups. UpSetR analysis depicts the intersection of ASVs between experimental groups. 'Persister' ASVs that remain throughout the experiment are marked in yellow, and potential 'recolonizers' transmitted from inoculum to recolonized sponges are marked in blue. The set size (number of ASVs) is shown in horizontal bars, the intersection size is shown in vertical bars above the respective intersection. The boxplot represents the ASV abundance as ln-transformed read counts.

sponge microbiomes separately. In the control treatment, 126 ASVs were correlated, and 81% of the bacteria-bacteria interactions were positive (Figure 4A). The four potential recolonizers, R1–R4, affected bacteria-bacteria interactions (Figure 4B). Recolonizers R1 and R2 had several interactions (9 and 10, respectively) with potential opportunistic ASVs that were not part of the untreated co-occurrence network at T0. Further, R1 and R2 had a positive correlation with each other. They were negatively correlated to other ASVs, including a highly abundant *Pseudoalteromonas* and a *Halodesulfovibrio*, likely opportunistic bacteria that were increasing after antibiotic treatment. The recolonized network was more complex than the control network with 16% more nodes and 28% more interactions, specifically 50% more negative and 15% more positive interactions.

DISCUSSION

In this study, we explored microbial community dynamics in the microbiome of the sponge *H. panicea* after disturbance by antibiotics and evaluated the potential for reversing changes via recolonization. Antibiotics exposure induced a strong dysbiosis that was characterized by higher relative and absolute abundances of opportunistic microbes and concomitantly, a reduced dominance of *Ca.* Halichondribacter symbioticus. Interestingly, the absolute abundances of *Ca.* H. symbioticus decreased only temporarily after antibiotic treatment and recovered to initial levels regardless of recolonization, implying a high stability and underlining the obligate nature of this sponge symbiont. Other symbionts most closely related to sponge- and other host-associated bacteria, also persisted in the microbiome in spite of the antibiotic treatment. Overall, dysbiosis resulted in more complex, but less specific bacteria-bacteria interactions than in untreated sponges. Recolonization with the natural microbiome had no effect on overall microbiome composition and diversity, but single bacterial taxa were transferred and successfully colonized the sponge. These recolonizers negatively affected the abundance of opportunistic bacteria, but the effects were not strong enough to recover the microbiome.

TABLE 1 Recolonization experiment: Affiliation and presence/absence of persistent ASVs, and potential recolonizers transmitted from inoculum to recolonized sponges.

Persister	Taxonomy	Presence T0	Presence T19 ctrl	Presence T19 recol	NCBI	Isolation source	Percent identity (%)	Query cover (%)	e-value	ASV
P1	Proteobacteria (*Halichondribacter*)	16/16	8/8	8/8	*Ca.* Halichondribacter symbioticus MH734183.1	*Halichondria panicea*	100	100	6 e-137	350235dc06427fbe808d1bb3452afc91
P2	Bacteroidota (*Cyclobacteriaceae*)	16/16	5/8	6/8	uncultured FJ393780.1	*Stichopus mollis* (echinoderm)	98.1	97	3 e-125	cdf31677e0019171c637774ded46a19d
P3	Proteobacteria (HOC36)	16/16	6/8	7/8	Gammaproteo-bacterium KT880336.1	*Hymeniacidon heliophila* (sponge)	94.4	100	6 e-112	5517e82f0118eaf02c2c08d15c54fd41
P4	Spirochaetota (*Spirochaetaceae*)	16/16	3/8	1/8	uncultured *Spirochaetales* FN424158.1	*Clathrina clathrus* (sponge)	90	92	4 e-84	b59335a4fffbb1846db5cfa20309b5a8
P5	Proteobacteria (*Vibrio*)	3/16	6/8	5/8	*Vibrio sp*. MT484171.1	*Hymeniacidon perlevis* (sponge)	100	100	6 e-137	5950c0e71fea54a0ea4a20b8a92357b5
P6	Nitrospirota (*Nitrospira*)	1/16	1/8	1/8	*Nitrospira sp*. JF802723.1	cold-water sponge	100	100	6 e-137	1594bb9f6e95a0b91bf7da9d083e55b3
P7	Bacteroidota (*Flavobacterium*)	2/16	5/8	6/8	uncultured HQ203853.1	seawater	100	100	6 e-137	838f2180a057d71e96a64cb64296df0b
P8	Proteobacteria (*Pseudoalteromonas*)	1/16	2/8	4/8	uncultured DQ274152.1	*Dysidea avara* (sponge)	97.4	100	3 e-125	cc9c276056e8a3d1292597378f5128da
P9	Proteobacteria (*Shewanella*)	4/16	5/8	8/8	*Shewanella sp*. KT583451.1	soft coral	100	100	6 e-137	3d56fd9774125a927d7e3142d542144f
P10	Proteobacteria (*Vibrio*)	2/16	6/8	5/8	*Vibrio sp*. MN974025.1	seawater	100	100	6 e-137	801f55a4831a1d3ba3eca43803ec88c3
P11	Bacteroidota (*Flavobacterium*)	1/16	5/8	3/8	*Flavobacteriaceae* DQ660391.1	sponge (Korea)	99.26	100	1 e-133	b5f8481ab1741f39cff72fb2289d7c7a
P12	Firmicutes (*Clostridiaceae*)	3/16	8/8	8/8	uncultured KP684471.1	*Halichondria panicea*	99.6	100	2 e-145	5b4a1fd9e459b1fe6de448175250ba66
P13	Proteobacteria (*Pseudoalteromonas*)	1/16	8/8	8/8	*Pseudoalteromonas sp*. CP041330.1	*Sycon capricorn* (sponge)	100	100	6 e-137	17753a04c358b65972ce4531833fcca1

Recolonizer	Taxonomy	Presence T0	Presence T19 ctrl	Presence T19 recol	NCBI	Isolation source	Percent identity (%)	Query cover (%)	e-value	ASV
R1	Bacteroidota (*Marinifiliaceae*)	0/8	0/8	8/8	uncultured KX172965.1	marine sediment	99.3	100	5 e-143	fcb9547cd146cb7db87c7405ac268abb
R2	Campilobacterota (*Arcobacter*)	0/8	0/8	7/8	*Arcobacter sp* AJ866949.1	marine sediment	99.6	97	8 e-142	19da1f623abc338a0fcca317fffdb984
R3	Campilobacterota (*Pseudoarcobacter*)	1/16	0/8	4/8	uncultured bacterium GU451405.1	macroalga	100	100	9 e-148	c463a879fa5cba0fca7210e19c696094
R4	Desulfobacteria (*Desulfofrigus*)	4/16	0/8	5/8	*Desulfofrigus* AJ630195.1	marine sediment	97.9	100	2 e-133	7ded0311410334d54b8dda089ef372db
R5	Gammaproteobacteria (*Vibrio*)	0/8	0/8	1/8	*Vibrio anguillarum* MK967051.1	*Aurelia aurita*	100	100	9 e-148	14f78e83791c069d499bdf618c7b7b73

(Continues)

TABLE 1 (Continued)

Recolonizer	Taxonomy	Presence T0	Presence T19 ctrl	Presence T19 recol	NCBI	Isolation source	Percent identity (%)	Query cover (%)	e-value	ASV
R6	Bacteroidota	0/8	0/8	1/8	uncultured bacterium AB779896	freshwater sediment	100	100	9 e-148	6dccb6b264cc78f903a9c11f80a3010a
R7	Bacteroidota (*Flavobacteriales*)	0/8	0/8	1/8	uncultured bacterium LC465504.1	seagrass	100	100	9 e-148	b74009ee162d508bac3435a12b73b0cd
R8	Gammaproteobacteria (*Thiotrichaceae*)	16/16	0/8	1/8	*Pelagibaculum spongiae* MG877746.1	*Halichondria panicea*	100	100	9 e-148	76df9929de34e15c00f74819ffd363ab

Note: Recolonizer in bold also appeared in *recolonized* bacterial co-occurrence network (Figure 4B). ASVs were compared to GenBank database (BLASTN) and the closest hit was reported.

Exposure to antibiotics promotes growth of opportunistic bacteria

We were unable to create gnotobiotic or aposymbiotic sponges, which is consistent with previous studies that have applied antibiotics in sponges so far (De Caralt et al., 2003; Friedrich et al., 2001; Gloeckner et al., 2013; Richardson et al., 2012; Schippers, 2013; Sipkema et al., 2003). In previous works, Schellenberg et al. could achieve a reduction of microbial load in *Haliclona cnidata* by continuous exposure to ampicillin and gentamycin over 4 weeks (Schellenberg et al., 2020). Contrary to our expectations, antibiotics resulted in an increase in total bacterial abundance in our study (Figure 2). Prolonged antibiotic exposure can favour the growth of antibiotic-resistant bacteria (Callens et al., 2018) as was indeed observed in our study (Figure S5) and would explain the increased carrying capacity. We cannot rule out the possibility that the sponge host was stressed by the antibiotic treatment, making it vulnerable to opportunistic bacteria that could consequently increase in numbers. Future efforts should thus include a set-up where phenotypic measures of the sponge performance (i.e., pumping activity) can be measured alongside.

Nevertheless, our antibiotic tests showed that all sponge-associated, culturable bacteria including those isolated from antibiotic treated sponges remained sensitive to rifampicin throughout the experiment. We thus speculate that these bacteria are protected by the sponge extracellular matrix that similar to mucus in the human gut or biofilms (Samad et al., 2019; Yan & Bassler, 2019) prevent antibiotics from reaching their bacterial target. Additionally, antibiotics are known to be less effective at high bacterial cell densities (Udekwu et al., 2009), which might further decrease their efficacy inside the sponge tissue. Completely eradicating sponge-associated bacteria by antibiotics continues to be a challenge and alternative methods like that is, rearing of sterile sponge larvae, reducing the microbiome via nutrient limitation or eradicating selected sponge symbionts by phage therapy should be explored. The advantages of sponge larvae over adult sponges are their higher surface to volume ratio and thus potential higher susceptibility to antibiotics, as well as their smaller bacterial community that needs to be eradicated. On the negative side, *H. panicea* is a temperate sponge species with a short reproductive season and consequently short window of opportunity for experimentation (Witte et al., 1994). Reduction of sponge-associated microbes under nutrient limitation was demonstrated unintentionally while a recirculating seawater aquarium system was tested to maintain *H. panicea* (Knobloch et al., 2019a). After 6 months, sponges had reduced their body mass but also their symbiont density including the dominant symbiont *Ca.* H. symbioticus. Manipulating food composition in the

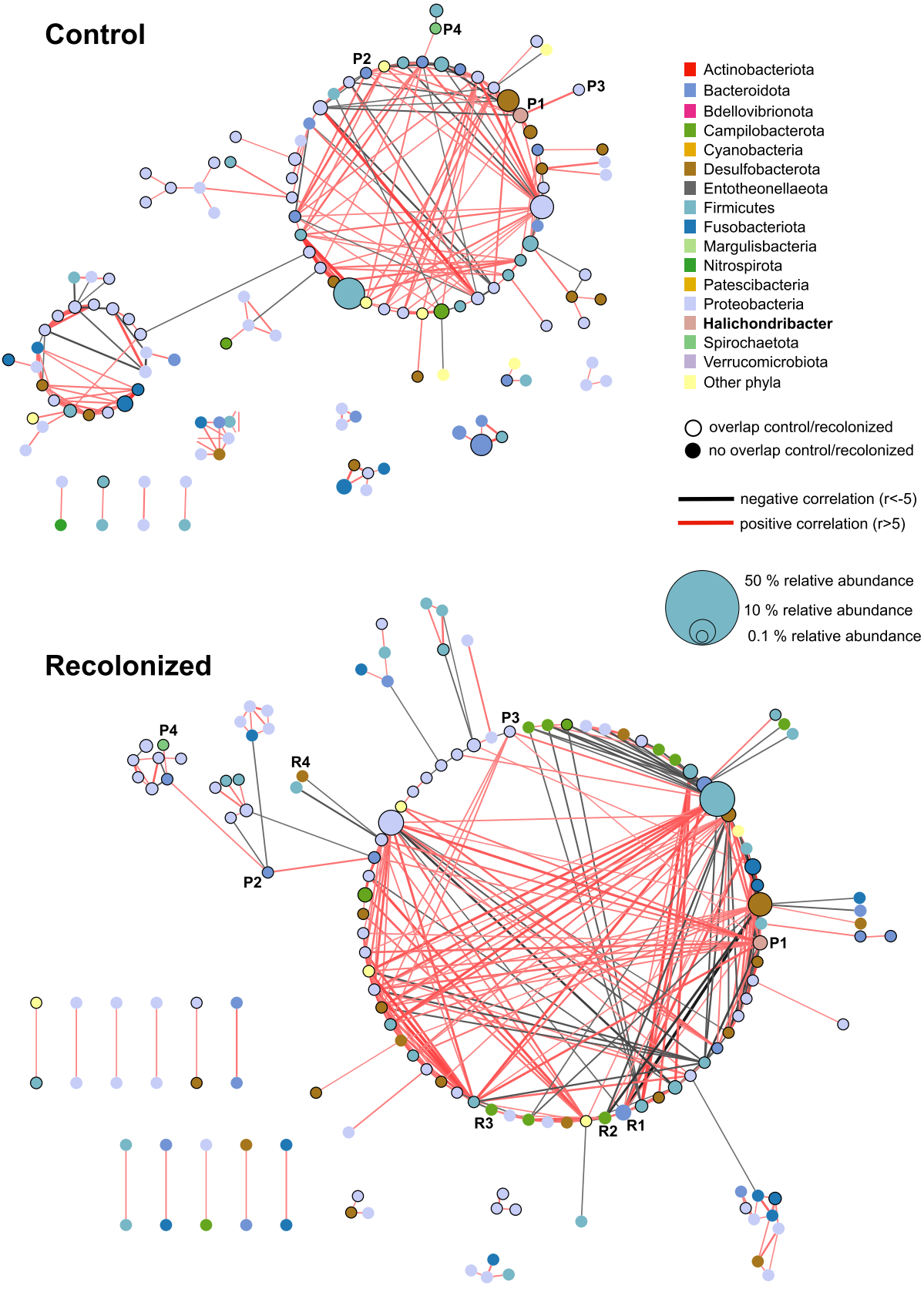

FIGURE 4 (A, B) Recolonization experiment: Bacterial co-occurrence networks for (A) control (T14–T19) and (B) recolonized *H. panicea* microbiomes (T14-T19). Co-occurrences between ASVs ($-0.5 > R > 0.5$, p-value <0.05) are displayed by edges (interactions) connecting nodes (ASVs). The colour of the edges depicts the direction of the correlation (negative or positive), and the thickness the interaction strength. The size of the nodes is proportional to the relative abundance of ASVs and the colour represents taxonomic affiliation. Nodes with a black outline are also present in the respective other treatment network. R1–R4 and P1–P4 indicate recolonizer and persister ASVs as defined in Table 1.

culture water could be a promising avenue to create *Ca.* H. symbioticus-free or strongly reduced sponges for experimentation without the use of antibiotics.

Ca. Halichondribacter symbioticus remains stable in spite of dysbiosis

The increase of antibiotic resistant, opportunistic bacteria correlated with a relative decrease of the dominant symbiont *Ca.* H. symbioticus (Figure 2C). In terms of absolute numbers however, *Ca.* H. symbioticus numbers remained surprisingly unaffected in most sponge individuals, and overall returned to initial levels regardless of recolonization (Figure 2B). Together with twelve other bacterial taxa, *Ca.* H. symbioticus comprises what we define as a 'persistent microbiome' that persisted throughout the experiment. Intriguingly, most persisters were related to sponge-associated microbes, providing strong evidence that these are true sponge symbionts (Table 1). In untreated sponges at T0, most persisters (P5-P13) appear to be part of the rare biosphere of the sponge as they occur at low relative abundances between 0.0045% and 0.02%. Since they were found in an increasing number of sponge individuals over time, it is conceivable that they grow inside of the sponge, which would however need to be verified by qPCR in future studies. Thus, their abundances are more dynamic and flexible than that of *Ca.* H. symbioticus which might reflect the different processes controlling their abundance. When looking at bacterial activity (i.e., qPCR on cDNA), we showed that at least the *Ca.* H. symbioticus clade remained transcriptionally active during dysbiosis. This finding is consistent with Schellenberg et al. (2020) who have described that a resilient portion of the sponge microbiome remains metabolically active after antibiotic treatment.

Surprisingly, the absolute abundance of *Ca.* H. symbioticus did not decrease in all sponge individuals. Inter-individual differences were detected by both *16 S* rRNA gene amplicon sequencing and qPCR (Figure S2). Genotyping sponges would elucidate whether host-genetics correlate to symbiont abundance, similarly as to what has been reported in humans (Tavalire et al., 2021). The low number of bacteria-bacteria interactions with the dominant symbiont in untreated sponge microbiomes let us speculate that *Ca.* H. symbioticus might be mainly host-dependent. One possible explanation could be that the hosts immune system controls symbiont abundance on an individual level. Indeed, *H. panicea* individuals differ in their expressed immune receptor repertoire, as well as in their transcriptional response to a microbial elicitor (Schmittmann et al., 2021). Whether such individual differences could be involved in controlling symbiont populations remains to be investigated. The symbiosis between *H. panicea* and its dominant symbiont is highly specific and may have evolved over evolutionarily long periods of time.

In terms of taxon level diversity, the *Ca.* Halichondribacter clade appears to be more diverse than previously appreciated (Knobloch et al., 2019a). Amplicon sequencing revealed a high diversity of ASVs classified as *Amylibacter*, which is the closest known clade related to *Ca.* H. symbioticus. Surprisingly, 15% of the interacting ASVs in untreated sponge microbiomes were associated to the *Amylibacter* family (Figure 2E). Some of those ASVs were highly similar to the *Ca.* H. symbioticus ASV (up to 99.6%), while others were less similar (>87%). An in-depth phylogenomic analysis of this extended sponge symbiont taxon would be required to understand the diversity and host-specificity of this conspicuous clade. When looking at full length *16 S* rRNA gene phylogenies, *Ca.* H. symbioticus is only distantly related to the genus *Amylibacter* (92.5%, unpublished data, Knobloch et al., 2019a), which leads us to speculate that the sponge symbiont lineage has diversified within its sponge host over evolutionary times. Whether and to what extent the phylogenetic differences translated into functional differences and adaptations remains to be investigated.

Dynamics and characteristics of dysbiosis

The application of antibiotics induced a strong disturbance of the sponge microbiome. The microbiome composition reached a new configuration consisting of increased bacterial abundance (Figure 2), reduced phylogenetic diversity, and higher evenness (Figure S4). Overall, the response on the bacterial community level to antibiotics was consistent between replicate sponges and also between experiments in terms of diversity and compositional changes. Similarly, in complex human gut communities, antibiotic exposure leads to a restructuring of the microbiome driven by antibiotic resistant, opportunistic bacteria (Francino, 2016; Gaulke et al., 2016) and can induce reversible but also long-lasting dysbioses (Lange et al., 2016). Increases in alpha- and beta diversity and compositional shifts towards opportunistic microbes are similar to environmental induced dysbiosis in other sponges (Lesser et al., 2016; Luter et al., 2012) and reviewed in (Pita et al., 2018).

Importantly, the combination of amplicon sequencing and qPCR in our study has been key to interpret the microbial patterns of dysbiosis. Without qPCR data, we would have concluded that *Ca.* H. symbioticus numbers were decreasing after antibiotic treatment. However, qPCR data clearly reveals that numbers of *Ca.* H. symbioticus remain constant whereas the microbiome shifts by an increased number of opportunists. Few studies reported bacterial change in absolute numbers during dysbiosis. As one example, increases in

absolute bacterial abundances were linked to disease in corals (Luna et al., 2010; Smith et al., 2015). Most other studies have so far relied on amplicon sequencing as a marker of relative community changes, although relative data alone can mask underlying community dynamics (Rao et al., 2021). Our study reiterates the importance to interpret microbial community shifts in the context of both, relative and absolute bacterial abundances.

Bacteria-bacteria interactions could be one important indicator of sponge microbiome condition and health. Indeed, changes in microbiome diversity and composition during dysbiosis were reflected in shifts of bacteria-bacteria co-occurrence networks. In untreated sponges, few ASVs had several bacteria-bacteria interactions (Figure 2), whereas the connectivity increased after disturbance (Figure 4). Similar patterns were observed in zebra fish microbiomes after exposure to antibiotics (Gaulke et al., 2016). We could clearly identify the loss of bacterial players (e.g., highly connected *Spirochaeta*) and the reduction of negative interactions during the transition from a untreated to a disturbed state. During dysbiosis, opportunistic *Pseudoalteromonas* were among the most abundant and connected ASVs and as such a potential drivers of microbiome dysbiosis. Crucial microbial players of sponge microbiome homeostasis in comparison to the transition to dysbiosis can be identified and might serve as indicators to predict microbiome stability and health, also in other host or environmental contexts (Tables S16–S18).

Single bacterial taxa recolonize with bacteria-bacteria interactions

Recolonization experiments of animal hosts are generally met with mixed success. In corals, the microbiome of antibiotic-treated animals was recovered by simple exposure to natural water (Bent et al., 2021). In another study, microbiome recolonization ("coral microbiome transplantation", CMT) of two coral species yielded a heat-resistant phenotype (Doering et al., 2021). However, one coral species was less susceptible to bacteria integration than the other. In our study, recolonization had no effect on the bacterial community composition and diversity and could not reverse the antibiotic-induced dysbiosis. One reason might be that the dysbiotic state is too stable for new bacteria to alter the community (Sommer et al., 2017). Another reason could be that the *H. panicea* symbionts cannot be transferred horizontally, for example, if they were vertically transmitted through the reproductive stages. It remains unclear why recolonization had no effect on the bacterial community composition. Yet, the successful transfer of single bacterial taxa opens a window of opportunity for recovery from dysbiosis.

Four bacterial taxa were transferred with the inoculum and consistently recolonized sponges (Figure 3, Table 1). In both recolonization experiments, transferred ASVs seem to establish with a delay after recolonization. Thus, potential changes on the community level might only become visible after a longer time than monitored in our experiments. The transferred taxa are affiliated to general marine bacteria and the question remains, whether they are opportunists that happen to benefit from the conditions in the sponge, or whether they would enable long-term restructuring of the healthy microbiome. Bacteria-bacteria co-occurrence networks on recolonized and control sponges indicate that transferred bacteria have strong, and partly negative correlations to other ASVs including those that became highly abundant after antibiotic treatment (Figure 4). Frequently negative, competitive correlations are related to network stability and thus homeostasis, through negative feedback loops (Coyte et al., 2015). Such negative interactions can be mediated by properties such as antimicrobial defence, host colonization and quorum sensing, which are frequently found on sponge symbiont genomes (Fan et al., 2012; Slaby et al., 2017). This stabilizing effect may be reflected in the intra-specific beta diversity that recovers to T0 levels after recolonization (Figure S4). This effect could provide for a mechanistic explanation for the general success of microbial recolonization/transplantation experiments in many different contexts ranging from faecal transplantation to coral probiotics.

Conclusions and outlook

This present study is among the first to experimentally manipulate marine sponge microbiomes by controlled experimentation in marine gnotobiotic chambers. We report the following findings: (i) The dominant symbiont in *H. panicea*, *Ca.* H. symbioticus, remained largely unchanged in spite of dysbiosis caused by growth of opportunistic bacteria following antibiotic treatment. This finding could only be uncovered by combination of quantitative (qPCR) with relative (amplicon sequencing) bacterial abundance analyses. (ii) Next to the dominant symbiont, several other ASVs were permanently associated with the sponge ('persisters') that are known from other sponge- and host-contexts. (iii) Recolonization of the sponge with its native microbiome did not reverse the microbiome from the dysbiotic state. Still, we discovered bacterial ASVs from the inoculum ('recolonizers') that could be successfully transferred. The purpose of choosing model species is to understand concepts that apply to a broader range of organisms that are less experimentally accessible. While we expect the results to be representative for other LMA sponges, future effort will need to explore whether these findings also apply to HMA sponges,

that have much denser and more diverse microbiomes. The present study contributes to ongoing efforts to unearthing mechanisms of microbiome dynamics and host-microbe as well as microbe-microbe interactions in the sponge holobiont.

AUTHOR CONTRIBUTIONS

L.S., L.P., S.F. and U.H. designed the study. Experiments were performed by L.S. and L.P. Molecular labwork was conducted by L.S. and antibiotic resistance tests were run by T.R. Bioinformaticanalyses was performed by L.S. and K.B., other analyses were done by L.S. The initialdraft of the manuscript was written by L. S., L.P. and U.H. and all authors participatedin writing later drafts.

ACKNOWLEDGEMENTS

We acknowledge Andrea Hethke and Ina Clefsen for technical assistance in the lab and the students Julius Krebs, Ashley Coons and Violeta Albacete for their experimental support. We thank Kristina Bayer and the CRC1182 community for stimulating discussions. We acknowledge the Competence Center for Genomic Analysis (CCGA) Kiel for amplicon sequencing. Further, we are grateful to Felix Mittermayer for sponge collections and to Claas Hiebenthal for technical support in the gnotobiotic chambers. Open Access funding enabled and organized by Projekt DEAL.

FUNDING INFORMATION

This project is supported by funding of the DFG (“Origin and Function of Metaorganisms”, CRC1182-TP B01) and the Gordon and Betty Moore Foundation (“Symbiosis in Aquatic Systems Initiative”, GBMF9352) to UH. LS is further supported by the International Max Planck Research School for Evolutionary Biology, and LP receives funding by the DFG (‘IMMUBASE’, 417,981,041) and is currently supported by ‘la Caixa’ Foundation (ID 10010434) and from the European Union’s Horizon 2020 research and innovation program under the Marie Sklodowska-Curie grand agreement No 847648, fellowship code is 104855.

CONFLICT OF INTEREST

The authors declare that the research was conducted in the absence of any commercial or financial relationships that could be construed as a potential conflict of interest.

DATA AVAILABILITY STATEMENT

All *16 S* rRNA gene amplicon reads and the sample metadata and attributes are available in the National Center for Biotechnology Information (NCBI) Sequence Read Archive (SRA): PRJNA786895; BioSample accessions: SAMN23732322- SAMN23732615.

REFERENCES

Althoff, K., Schütt, C., Steffen, R., Batel, R. & Müller, W.E.G. (1998) Evidence for a symbiosis between bacteria of the genus *Rhodobacter* and the marine sponge *Halichondria panicea*: harbor also for putatively toxic bacteria? *Marine Biology*, 130, 529–536.

Amano, S. (1986) Larval release in response to a light signal by the intertidal sponge *Halichondria panicea*. *The Biological Bulletin*, 171, 371–378.

Augustin, R., Fraune, S., Franzenburg, S. & Bosch, T.C.G. (2012) In: Mylonakis, E., Ausubel, F.M., Gilmore, M. & Casadevall, A. (Eds.) *Recent advances on model hosts*. New York, NY: Springer.

Barthel, D. (1986) On the ecophysiology of the sponge *Halichondria panicea* in Kiel bight. I. Substrate specificity, growth and reproduction. *Marine Ecology Progress Series*, 32, 291–298.

Barthel, D. (1988) On the ecophysiology of the sponge *Halichondria panicea* in Kiel bight. II. Biomass, production, energy budget and integration in environmental processes. *Marine Ecology*, 43, 87–93.

Bayer, K., Kamke, J. & Hentschel, U. (2014) Quantification of bacterial and archaeal symbionts in high and low microbial abundance sponges using real-time PCR. *FEMS Microbiology Ecology*, 89, 679–690.

Bell, J.J. (2008) The functional roles of marine sponges. *Estuarine, Coastal and Shelf Science*, 79, 341–353.

Bell, J.J., Bennett, H.M., Rovellini, A. & Webster, N.S. (2018) Sponges to be winners under near-future climate scenarios. *Bioscience*, 68, 955–968.

Bent, S.M., Miller, C.A., Sharp, K.H., Hansel, C.M. & Apprill, A. (2021) Differential patterns of microbiota recovery in symbiotic and aposymbiotic corals following antibiotic disturbance. *mSystems*, 6, 1–18.

Blanquer, A., Uriz, M.J., Cebrian, E. & Galand, P.E. (2016) Snapshot of a bacterial microbiome shift during the early symptoms of a massive sponge die-offin the western Mediterranean. *Frontiers in Microbiology*, 7, 1–10.

Bolyen, E., Rideout, J.R., Dillon, M.R., Bokulich, N.A., Abnet, C.C., Al-Ghalith, G.A. et al. (2019) Reproducible, interactive, scalable and extensible microbiome data science using QIIME 2. *Nature Biotechnology*, 37, 852–857.

Bosch, T.C.G., Guillemin, K. & McFall-Ngai, M. (2019) Evolutionary “experiments” in symbiosis: the study of model animals provides insights into the mechanisms underlying the diversity of host–microbe interactions. *BioEssays*, 41, 1–8.

Britstein, M., Cerrano, C., Burgsdorf, I., Zoccarato, L., Kenny, N.J., Riesgo, A. et al. (2020) Sponge microbiome stability during environmental acquisition of highly specific photosymbionts. *Environmental Microbiology*, 22, 3593–3607.

Bucher, M., Wolfowicz, I., Voss, P.A., Hambleton, E.A. & Guse, A. (2016) Development and symbiosis establishment in the cnidarian endosymbiosis model *Aiptasia sp*. *Scientific Reports*, 6, 1–11.

Busch, K., Slaby, B.M., Bach, W., Boetius, A., Clefsen, I., Colaço, A. et al. (2022) Biodiversity, environmental drivers, and sustainability of the global deep-sea sponge microbiome. *Nature Communications*, 13, 5160.

Callahan, B.J., McMurdie, P.J., Rosen, M.J., Han, A.W., Johnson, A. J.A. & Holmes, S.P. (2016) DADA2: high-resolution sample inference from Illumina amplicon data. *Nature Methods*, 13, 581–583.

Callens, M., Watanabe, H., Kato, Y., Miura, J. & Decaestecker, E. (2018) Microbiota inoculum composition affects holobiont assembly and host growth in *daphnia*. *Microbiome*, 6, 56.

Campana, S., Demey, C., Busch, K., Hentschel, U., Muyzer, G. & De Goeij, J.M. (2021) Marine sponges maintain stable bacterial communities between reef sites with different coral to algae cover ratios. *FEMS Microbiology Ecology*, 97, 1–12.

De Caralt, S., Agell, G. & Uriz, M.J. (2003) Long-term culture of sponge explants: conditions enhancing survival and growth, and assessment of bioactivity. *Biomolecular Engineering*, 20, 339–347.

Cerrano, C., Giovine, M. & Steindler, L. (2022) *Petrosia ficiformis* (Poiret, 1789): an excellent model for holobiont and biotechnological studies. *Current Opinion in Biotechnology*, 74, 61–65.

Cho, I. & Blaser, M.J. (2012) The human microbiome: At the interface of health and disease. *Nature Reviews. Genetics*, 13, 260–270.

Conway, J.R., Lex, A. & Gehlenborg, N. (2017) UpSetR: an R package for the visualization of intersecting sets and their properties. *Bioinformatics*, 33, 2938–2940.

Costa, R.M., Cárdenas, A., Loussert-Fonta, C., Toullec, G., Meibom, A. & Voolstra, C.R. (2021) Surface topography, bacterial carrying capacity, and the prospect of microbiome manipulation in the sea anemone coral model *Aiptasia*. *Frontiers in Microbiology*, 12, 1–16.

Costello, E.K., Stagaman, K., Dethlefsen, L., Bohannan, B.J.M. & Relman, D.A. (2012) The application of ecological theory toward an understanding of the human microbiome. *Science*, 336, 1255–1262.

Coyte, K.Z., Schluter, J. & Foster, K.R. (2015) The ecology of the microbiome: networks, competition, and stability. *Science*, 350, 663–666.

Doering, T., Wall, M., Putchim, L., Rattanawongwan, T., Schroeder, R., Hentschel, U. et al. (2021) Towards enhancing coral heat tolerance: a "microbiome transplantation" treatment using inoculations of homogenized coral tissues. *Microbiome*, 9, 102.

Domin, H., Zurita-Gutiérrez, Y.H., Scotti, M., Buttlar, J., Hentschel, U. & Fraune, S. (2018) Predicted bacterial interactions affect *in vivo* microbial colonization dynamics in *Nematostella*. *Frontiers in Microbiology*, 9, 728.

Douglas, A.E. (2019) Simple animal models for microbiome research. *Nature Reviews. Microbiology*, 17, 764–775.

Easson, C.G. & Thacker, R.W. (2014) Phylogenetic signal in the community structure of host-specific microbiomes of tropical marine sponges. *Frontiers in Microbiology*, 5, 1–11.

Erpenbeck, D., Knowlton, A.L., Talbot, S.L., Highsmith, R.C. & Van Soest, R.W. (2004) A molecular comparison of Alaskan and Northeast Atlantic *Halichondria panicea* (Pallas 1766) (Porifera: Demospongiae) populations. *Bollettino dei Musei e degli Istituti biologici dell'Università di Genova*, 61, 319–325.

Fan, L., Liu, M., Simister, R., Webster, N.S. & Thomas, T. (2013) Marine microbial symbiosis heats up: the phylogenetic and functional response of a sponge holobiont to thermal stress. *The ISME Journal*, 7, 991–1002.

Fan, L., Reynolds, D., Liu, M., Stark, M., Kjelleberg, S., Webster, N.S. & Thomas, T. (2012) Functional equivalence and evolutionary convergence in complex communities of microbial sponge symbionts. *Proceedings of the National Academy of Sciences*, 109, E1878–E1887.

Fierer, N., Ferrenberg, S., Flores, G.E., González, A., Kueneman, J., Legg, T. et al. (2012) From animalcules to an ecosystem: application of ecological concepts to the human microbiome. *Annual Review of Ecology, Evolution, and Systematics*, 43, 137–155.

Francino, M.P. (2016) Antibiotics and the human gut microbiome: Dysbioses and accumulation of resistances. *Frontiers in Microbiology*, 6, 1–11.

Franzenburg, S., Fraune, S., Künzel, S., Baines, J.F., Domazet-Loso, T. & Bosch, T.C.G. (2012) MyD88-deficient *hydra* reveal an ancient function of TLR signaling in sensing bacterial colonizers. *Proc Natl Acad Sci U S A*, 47, 19374–19379.

Friedman, J. & Alm, E.J. (2012) Inferring correlation networks from genomic survey data. *PLoS Computational Biology*, 8, 1–11.

Friedrich, A.B., Fischer, I. & Proksch, P. (2001) Temporal variation of the microbial community associated with the mediterranean sponge *Aplysina aerophoba*. *FEMS Microbiology Ecology*, 38, 105–113.

Gaulke, C.A., Barton, C.L., Proffitt, S., Tanguay, R.L. & Sharpton, T.J. (2016) Triclosan exposure is associated with rapid restructuring of the microbiome in adult zebrafish. *PLoS One*, 11, 1–20.

Gloeckner, V., Lindquist, N., Schmitt, S. & Hentschel, U. (2013) *Ectyoplasia ferox*, an experimentally tractable model for vertical microbial transmission in marine sponges. *Microbial Ecology*, 65, 462–474.

Gloeckner, V., Wehrl, M., Moitinho-silva, L., Schupp, P., Pawlik, J.R., Lindquist, N.L. et al. (2014) The HMA-LMA dichotomy revisited: an electron microscopical survey of 56 sponge species. *The Biological Bulletin*, 227, 78–88.

Ianiro, G., Segal, J.P., Mullish, B.H., Quraishi, M.N., Porcari, S., Fabiani, G. et al. (2020) Fecal microbiota transplantation in gastrointestinal and extraintestinal disorders. *Future Microbiology*, 15, 1173–1186.

Knobloch, S., Jóhannsson, R. & Marteinsson, V. (2019a) Bacterial diversity in the marine sponge *Halichondria panicea* from Icelandic waters and host-specificity of its dominant symbiont "*Candidatus* Halichondribacter symbioticus". *FEMS Microbiology Ecology*, 95, 1–13.

Knobloch, S., Jóhannsson, R. & Marteinsson, V. (2019b) Co-cultivation of the marine sponge *Halichondria panicea* and its associated microorganisms. *Scientific Reports*, 9, 1–11.

Knobloch, S., Jóhannsson, R. & Marteinsson, V. (2019c) Genome analysis of sponge symbiont "*Candidatus* Halichondribacter symbioticus" shows genomic adaptation to a host-dependent lifestyle. *Environmental Microbiology*, 22, 483–498.

Kozich, J.J., Westcott, S.L., Baxter, N.T., Highlander, S.K. & Schloss, P.D. (2013) Development of a dual-index sequencing strategy and curation pipeline for analyzing amplicon sequence data on the miseq illumina sequencing platform. *Applied and Environmental Microbiology*, 79, 5112–5120.

Kumala, L., Larsen, M., Glud, R.N. & Canfield, D.E. (2021) Spatial and temporal anoxia in single-osculum *Halichondria panicea* demosponge explants studied with planar optodes. *Marine Biology*, 168, 1–13.

Lange, K., Buerger, M., Stallmach, A. & Bruns, T. (2016) Effects of antibiotics on gut microbiota. *Digestive Diseases*, 34, 260–268.

Lavrov, A.I. & Kosevich, I.A. (2016) Sponge cell reaggregation: cellular structure and morphogenetic potencies of multicellular aggregates. *Journal of Experimental Zoology Part A: Ecological Genetics*, 325, 158–177.

Le Bastard, Q., Ward, T., Sidiropoulos, D., Hillmann, B.M., Chun, C. L., Sadowsky, M.J. et al. (2018) Fecal microbiota transplantation reverses antibiotic and chemotherapy-induced gut dysbiosis in mice. *Scientific Reports*, 8, 1–11.

Leigh, B.A., Liberti, A. & Dishaw, L.J. (2016) Generation of germ-free *Ciona intestinalis* for studies of gut-microbe interactions. *Frontiers in Microbiology*, 7, 1–8.

Lesser, M.P., Fiore, C., Slattery, M. & Zaneveld, J. (2016) Climate change stressors destabilize the microbiome of the Caribbean barrel sponge, *Xestospongia muta*. *Journal of Experimental Marine Biology and Ecology*, 475, 11–18.

Li, C.W., Chen, J.Y. & Hua, T.E. (1998) Precambrian sponges with cellular structures. *Science*, 279, 879–882.

Luna, G.M., Bongiorni, L., Gili, C., Biavasco, F. & Danovaro, R. (2010) *Vibrio harveyi* as a causative agent of the white syndrome in tropical stony corals. *Environmental Microbiology Reports*, 2, 120–127.

Lüskow, F., Kløve-Mogensen, K., Tophøj, J., Pedersen, L.H., Riisgård, H.U. & Eriksen, N.T. (2019b) Seasonality in lipid content of the demosponges *Halichondria panicea* and *H. bowerbanki* at two study sites in temperate Danish waters. *Frontiers in Marine Science*, 6, 1–7.

Lüskow, F., Riisgård, H.U., Solovyeva, V. & Brewer, J.R. (2019a) Seasonal changes in bacteria and phytoplankton biomass

control the condition index of the demosponge *Halichondria panicea* in temperate Danish waters. *Marine Ecology Progress Series*, 608, 119–132.

Luter, H.M., Bannister, R.J., Whalan, S., Kutti, T., Pineda, M.C. & Webster, N.S. (2017) Microbiome analysis of a disease affecting the deep-sea sponge *Geodia barretti*. *FEMS Microbiology Ecology*, 93, 1–6.

Luter, H.M., Whalan, S. & Webster, N.S. (2012) Thermal and sedimentation stress are unlikely causes of brown spot syndrome in the coral reef sponge, *Ianthella basta*. *PLoS One*, 7, 1–9.

Manor, O., Dai, C.L., Kornilov, S.A., Smith, B., Price, N.D., Lovejoy, J. C. et al. (2020) Health and disease markers correlate with gut microbiome composition across thousands of people. *Nature Communications*, 11, 1–12.

Mauri, M., Elli, T., Caviglia, G., Uboldi, G. & Azzi, M. (2017) RAW-Graphs: A visualisation platform to create open outputs. *ACM International Conference Proceeding*, 28, 5.

Moitinho-Silva, L., Steinert, G., Nielsen, S., Hardoim, C.C.P., Wu, Y. C., McCormack, G.P. et al. (2017) Predicting the HMA-LMA status in marine sponges by machine learning. *Frontiers in Microbiology*, 8, 1–14.

Mortzfeld, B.M., Urbanski, S., Reitzel, A.M., Künzel, S., Technau, U. & Fraune, S. (2016) Response of bacterial colonization in *Nematostella vectensis* to development, environment and biogeography. *Environmental Microbiology*, 18, 1764–1781.

Naim, M.A., Morillo, J.A., Sørensen, S.J., Waleed, A.A.S., Smidt, H. & Sipkema, D. (2014) Host-specific microbial communities in three sympatric North Sea sponges. *FEMS Microbiology Ecology*, 90, 390–403.

Ng, K.M., Ferreyra, J.A., Higginbottom, S.K., Lynch, J.B., Kashyap, P. C., Gopinath, S. et al. (2013) Microbiota-liberated host sugars facilitate post-antibiotic expansion of enteric pathogens. *Nature*, 502, 96–99.

Nyholm, S.V. & McFall-Ngai, M.J. (2021) A lasting symbiosis: how the Hawaiian bobtail squid finds and keeps its bioluminescent bacterial partner. *Nature Reviews. Microbiology*, 19, 666–679.

Peixoto, R.S., Harkins, D.M. & Nelson, K.E. (2021) Advances in microbiome research for animal health. *Annual Review of Animal Biosciences*, 9, 289–311.

Pita, L., Fraune, S. & Hentschel, U. (2016) Emerging sponge models of animal-microbe symbioses. *Frontiers in Microbiology*, 7, 1–8.

Pita, L., Rix, L., Slaby, B.M., Franke, A. & Hentschel, U. (2018) The sponge holobiont in a changing ocean: from microbes to ecosystems. *Microbiome*, 6, 46.

Pleasants, J.R. (1959) Rearing germfree rats, mice, and rabbits. *Annals of the New York Academy of Sciences*, 78, 116–126.

Posadas, N., Baquiran, J.I.P., Nada, M.A.L., Kelly, M. & Conaco, C. (2021) Microbiome diversity and host immune functions in fl uence survivorship of sponge holobionts under future ocean conditions. *The ISME Journal*, 16, 58–67.

Quast, C., Pruesse, E., Yilmaz, P., Gerken, J., Schweer, T., Yarza, P. et al. (2013) The SILVA ribosomal RNA gene database project: improved data processing and web-based tools. *Nucleic Acids Research*, 41, 590–596.

Rao, C., Coyte, K.Z., Bainter, W., Geha, R.S., Martin, C.R. & Rakoff-Nahoum, S. (2021) Multi-kingdom ecological drivers of microbiota assembly in preterm infants. *Nature*, 591, 633–638.

Richardson, C., Hill, M., Marks, C., Runyen-Janecky, L. & Hill, A. (2012) Experimental manipulation of sponge/bacterial symbiont community composition with antibiotics: sponge cell aggregates as a unique tool to study animal/microorganism symbiosis. *FEMS Microbiology Ecology*, 81, 407–418.

Riisgård, H.U., Kumala, L. & Charitonidou, K. (2016) Using the F/R-ratio for an evaluation of the ability of the demosponge *Halichondria panicea* to nourish solely on phytoplankton versus free-living bacteria in the sea. *Marine Biology Research*, 12, 907–916.

Robles-Vera, I., Toral, M., de la Visitación, N., Sánchez, M., Gómez-Guzmán, M., Romero, M. et al. (2020) Probiotics prevent dysbiosis and the rise in blood pressure in genetic hypertension: role of short-chain fatty acids. *Molecular Nutrition & Food Research*, 64, 1–13.

Rooks, M.G., Veiga, P., Wardwell-Scott, L.H., Tickle, T., Segata, N., Michaud, M. et al. (2014) Gut microbiome composition and function in experimental colitis during active disease and treatment-induced remission. *The ISME Journal*, 8, 1403–1417.

Samad, T., Co, J.Y., Witten, J. & Ribbeck, K. (2019) Mucus and mucin environments reduce the efficacy of polymyxin and fluoroquinolone antibiotics against *Pseudomonas aeruginosa*. *ACS Biomaterials Science & Engineering*, 5, 1189–1194.

Sarker, S.A., Ahmed, T. & Brüssow, H. (2017) Persistent diarrhea: a persistent infection with enteropathogens or a gut commensal dysbiosis? *Environmental Microbiology*, 19, 3789–3801.

Schellenberg, J., Reichert, J., Hardt, M., Klingelhöfer, I., Morlock, G., Schubert, P. et al. (2020) The bacterial microbiome of the long-term aquarium cultured high-microbial abundance sponge *Haliclona cnidata* – sustained bioactivity despite community shifts under detrimental conditions. *Frontiers in Marine Science*, 7, 266.

Schippers, K.J. (2013) *Sponge cell culture*. Netherlands: Wageningen Universtiy.

Schmittmann, L., Franzenburg, S. & Pita, L. (2021) Individuality in the immune repertoire and induced response of the sponge *Halichondria panicea*. *Frontiers in Immunology*, 12, 1–13.

Schmittmann, L. & Hentschel, U. (2021) Antibiotic treatment of the sponge *Halichondria panicea* and subsequent recolonization V2. *Protocols.io*. https://doi.org/10.17504/protocols.io.3byl4kpk2vo5/v2

Schmittmann, L. & Pita, L. (2021) DNA/RNA extraction and qPCR protocol to assess bacterial abudnance in the sponge *Halichondria panicea*. *Protocols.io*. https://doi.org/10.17504/protocols.io.bxwwppfe

Segata, N., Izard, J., Waldron, L., Gevers, D., Miropolsky, L., Garrett, W.S. et al. (2011) Metagenomic biomarker discovery and explanation. *Genome Biology*, 12, R60.

Shaffer, M., Thurimella, K., Sterrett, J. D. & Lozupone, C.A. (2020) SCNIC: sparse correlation network investigation for compositional data. *Molecular Ecology Resources*, 1–14.

Shannon, P., Markiel, A., Ozier, O., Baliga, N.S., Wang, J.T., Ramage, D. et al. (2003) Cytoscape: A software environment for integrated models of biomolecular interaction networks. *Genome Research*, 13, 2498–2504.

Sipkema, D., Tramper, J., van Wielink, R., van Lammeren, A.A.M., Osinga, R., & Wijffels, R.H. (2003) Primmorphs from seven marine sponges: formation and structure. *Journal of Biotechnology*, 100, 127–139.

Slaby, B.M., Hackl, T., Horn, H., Bayer, K. & Hentschel, U. (2017) Metagenomic binning of a marine sponge microbiome reveals unity in defense but metabolic specialization. *The ISME Journal*, 11, 2465–2478.

Smith, D., Leary, P., Craggs, J., Bythell, J. & Sweet, M. (2015) Microbial communities associated with healthy and white syndrome-affected *Echinopora lamellosa* in aquaria and experimental treatment with the antibiotic ampicillin. *PLoS One*, 10, 1–17.

Sommer, F., Anderson, J.M., Bharti, R., Raes, J. & Rosenstiel, P. (2017) The resilience of the intestinal microbiota influences health and disease. *Nature Reviews. Microbiology*, 15, 630–638.

Steinert, G., Rohde, S., Janussen, D., Blaurock, C. & Schupp, P.J. (2017) Host-specific assembly of sponge-associated prokaryotes at high taxonomic ranks. *Scientific Reports*, 7, 1–9.

Strati, F., Pujolassos, M., Burrello, C., Giuffrè, M.R., Lattanzi, G., Caprioli, F. et al. (2021) Antibiotic-associated dysbiosis affects the ability of the gut microbiota to control intestinal inflammation

upon fecal microbiota transplantation in experimental colitis models. *Microbiome*, 9, 1–15.

Strehlow, B.W., Schuster, A., Francis, W.R. & Canfield, D.E. (2022) Metagenomic data for *Halichondria panicea* from Illumina and Nanopore sequencing and preliminary genome assemblies for the sponge and two microbial symbionts. *BMC Research Notes*, 15, 135.

Tavalire, H.F., Christie, D.M., Leve, L.D., Ting, N., Cresko, W.A. & Bohannan, B.J.M. (2021) Shared environment and genetics shape the gut microbiome after infant adoption. *MBio*, 12, e00548–e00521.

Thomas, T., Moitinho-Silva, L., Lurgi, M., Björk, J.R., Easson, C., Astudillo-García, C. et al. (2016) Diversity, structure and convergent evolution of the global sponge microbiome. *Nature Communications*, 7, 11870.

Udekwu, K.I., Parrish, N., Ankomah, P., Baquero, F. & Levin, B.R. (2009) Functional relationship between bacterial cell density and the efficacy of antibiotics. *The Journal of Antimicrobial Chemotherapy*, 63, 745–757.

Vad, J., Dunnett, F., Liu, F., Montagner, C.C., Roberts, J.M. & Henry, T.B. (2020) Soaking up the oil: biological impacts of dispersants and crude oil on the sponge *Halichondria panicea*. *Chemosphere*, 257, 127109.

Visick, K.L., Stabb, E.V. & Ruby, E.G. (2021) A lasting symbiosis: how *Vibrio fischeri* finds a squid partner and persists within its natural host. *Nature Reviews. Microbiology*, 19, 654–665.

Wehrl, M., Steinert, M. & Hentschel, U. (2007) Bacterial uptake by the marine sponge *Aplysina aerophoba*. *Microbial Ecology*, 53, 355–365.

Weiland-Bräuer, N., Neulinger, S.C., Pinnow, N., Kunzel, S., Baines, J.F. & Schmitz, R.A. (2015) Composition of bacterial communities associated with *Aurelia aurita* changes with compartment, life stage, and population. *Applied and Environmental Microbiology*, 81, 6038–6052.

Wichels, A., Würtz, S., Döpke, H., Schütt, C. & Gerdts, G. (2006) Bacterial diversity in the breadcrumb sponge *Halichondria panicea* (Pallas). *FEMS Microbiology Ecology*, 56, 102–118.

Witte, U., Barthel, D. & Tendal, O. (1994) The reproductive cycle of the sponge *Halichondria panicea* Pallas (1766) and its relationship to temperature and salinity. *Journal of Experimental Marine Biology and Ecology*, 183, 41–52.

Yan, J. & Bassler, B.L. (2019) Surviving as a community: antibiotic tolerance and persistence in bacterial biofilms. *Cell Host & Microbe*, 26, 15–21.

SUPPORTING INFORMATION

Additional supporting information can be found online in the Supporting Information section at the end of this article.

How to cite this article: Schmittmann, L., Rahn, T., Busch, K., Fraune, S., Pita, L. & Hentschel, U. (2022) Stability of a dominant sponge-symbiont in spite of antibiotic-induced microbiome disturbance. *Environmental Microbiology*, 24(12), 6392–6410. Available from: https://doi.org/10.1111/1462-2920.16249